Chemical Science

ROYAL SOCIETY OF CHEMISTRY

EDGE ARTICLE

View Article Online
View Journal

Cite this: DOI: 10.1039/d6sc01056c

All publication charges for this article have been paid for by the Royal Society of Chemistry

Xanthene-to-fluorene skeletal editing *via* oxygen deletion mediated by boron and aluminium radicals

Emily Nahon, [a] Gareth R. Nelmes, [a] Elena Dallerba, [b] Li Feng Lim, [a] Nicholas Cox, [a] Claire L. McMullin, [c] Massimiliano Massi, [b] Fabian Kallmeier *[a] and Jamie Hicks *[a]

Received 6th February 2026
Accepted 17th April 2026

DOI: 10.1039/d6sc01056c

rsc.li/chemical-science

Single-atom skeletal editing *via* selective oxygen deletion from diarylethers remains an underdeveloped transformation, despite its potential to directly access new carbon frameworks. Here, we report a boron- and aluminium-mediated *O*-deletion reaction that converts xanthene and diphenylether motifs into fluorene and biphenyl architectures through concomitant C–C bond formation. Lithium metal reduction of diamido arylether boron halides affords lithium boryloxy complexes in high yield and on a multigram scale, with both the new C–C bond and terminal B–O$^-$ unit formed in a single step *via* a transient open-shell B(II) intermediate. Hydrolysis furnishes fluorene- and biphenyl-based [1,3,2]diazaborepin-2-ols, representing previously inaccessible boron-containing fluorophores that exhibit high photoluminescence quantum yields. Extension of this strategy to aluminium allows clean hydrolytic release of the organic scaffold and provides a concise, scalable synthesis of functionalised 4,5-diaminofluorenes. These results establish *O*-deletion as a viable skeletal editing strategy for arylethers and highlight the role of main-group radical intermediates in selective framework reorganisation.

Introduction

Skeletal editing, *i.e.,* the selective alteration of a molecule's core motif, typically by a single atom, has recently experienced a surge in popularity and is now an invaluable tool in contemporary synthetic chemistry. Sarpong, Levin, and coworkers have recently suggested a classification scheme for single-atom skeletal edits.[1] The methods currently in use typically revolve around privileged structures in medicinal chemistry,[2,3] *e.g.* pyridine to benzene[4–7] and *vice versa*,[8] isothiazole to pyrazole,[9] or removing nitrogen atoms from dialkylamines.[10] One example of single-atom skeletal editing that is less developed is the oxygen-deletion reaction in ethers, which would yield a new C–C bond. Such a reaction would be expected to proceed through a reductive pathway, eliminating "O^{2-}". However, the reduction of diarylethers to the corresponding biaryls (and cyclic analogues) is hampered by the non-selective reaction with alkali metals – including the low tolerance of functional groups – and the need for subsequent C–C coupling of the individual fragments (Fig. 1, top).[11–16]

In 2024, Frenking, Driess and coworkers demonstrated how coordination chemistry could aid in this regard (Fig. 1, centre).[17] The team showed that the 9,10-diboraphenanthrene motif in

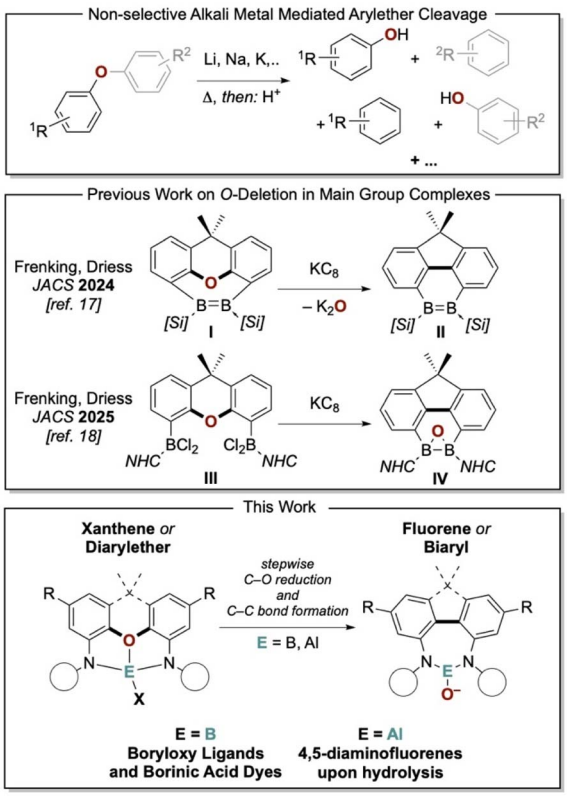

Fig. 1 (Top) challenging selectivity in alkali metal-mediated diarylether cleavage. (Middle) current state-of-the-art of skeletal editing in main-group chemistry; [Si] = *N*-heterocyclic silylene [{PhC(N*t*Bu)$_2$} (Me$_2$N)Si], NHC = [C{N(iPr)CMe}$_2$]. (Bottom) this work. Selective *O*-deletion reaction in diamido-xanthene/-diarylether boron complexes upon reduction *via* alkali metals.

[a]*Research School of Chemistry, Australian National University, Sullivans Creek Rd, Acton, ACT, 2601, Australia. E-mail: fabian.kallmeier@anu.edu.au; jamie.hicks@anu.edu.au*

[b]*School of Molecular and Life Sciences (MLS), Curtin University, 500 Townsing Dr, Bentley, WA 6102, Australia*

[c]*Department of Chemistry, University of Bath, Claverton Down, Bath, BA2 7AY, UK*

(**II**) could be prepared selectively *via* the reductive ring contraction of 4,5-([Si]B)$_2$-xanthene ([Si] = {PhC(N*t*Bu)$_2$}(Me$_2$N)Si) (**I**) by reduction with potassium graphite (KC_8), with the oxygen atom suggested to be eliminated as K_2O.[17] Similarly, the same groups observed a related rearrangement upon treatment of xanthene-4,5-diyl-bis(dichloroborane) (**III**), in which an *N*-heterocyclic carbene is coordinated to each boron centre, with KC_8. In this case, diboraoxirane (**IV**) could be obtained, which was shown to undergo ring expansion upon reaction with an array of small molecules, *e.g.*, CO_2, O_2, and S_8.[18]

In this work, we demonstrate a selective *O*-deletion reaction from diamido boron and aluminium compounds bearing a diarylether backbone (Fig. 1, bottom). The procedure remains selective even on a multigram scale and allows for the synthesis of diverse products, including synthetically challenging 4,5-substituted fluorenes and novel boron-based fluorescent dyes.

Results and discussion

With the chemistry of **I** and **III** demonstrating general feasibility, we initially set out to synthesise diamidoxanthene-based diamido boron fluoride **1-F**, as shown in Fig. 2. **1-F** was obtained cleanly by deprotonation of H$_2$(**NON**) (**NON**: 4,5-bis(2,6-diisopropylanilido)-2,7-di-*tert*-butyl-9,9-dimethylxanthene) using two equivalents of *n*-BuLi as the base, followed by subsequent salt metathesis with $BF_3{\cdot}OEt_2$. The target compound, which is air- and moisture-stable, was obtained in 69% crystalline yield on a 5 g scale (see SI for synthetic details). **1-F** was conveniently converted to the analogous bromide **1-Br** in 72% yield by stirring with an excess of BBr_3 in toluene at room temperature for 2 days.[19] The compounds were characterised by multinuclear NMR spectroscopy, and their solid-state structures were confirmed by X-ray diffraction (Fig. 2, bottom).

With suitable precursors in hand, our attention turned to their behaviour under reductive conditions (Fig. 3, top). A d_8-THF solution of **1-F** with a small piece of lithium ribbon was sonicated at ambient temperature in an air-tight NMR tube. Reaction progression was indicated by the appearance of a fluorescent yellow-coloured solution, which was complete after 24 hours, as indicated by NMR analysis. ^{11}B-NMR spectroscopy showed a single new boron-containing product, with a slight shift compared to that of the starting material (20.5 ppm *cf.* 21.8 ppm for **1-F**). In addition, the disappearance of a signal in ^{19}F-NMR spectrum indicated the loss of the fluoride ligand. Multigram quantities of the same product were obtained by sonicating a flask containing **1-F** and lithium ribbon overnight, followed by stirring the reaction mixture for 2 days at 60 °C, or by stirring a THF solution of **1-F** over finely divided Li metal on LiCl (or LiBr) at room temperature overnight.[20]

Crystals suitable for X-ray diffraction were grown from a concentrated benzene solution of the new product and showed it to be the lithium boryloxy **3-OLi** (Fig. 3). Boryloxy compounds are boron(III) compounds featuring a B–O$^-$ moiety, and have gained significant attention over the last years as strong σ- and π-donor ligands.[21–32] Complex **3-OLi** consists of a 3-coordinate boron(III) centre, which, contrary to its progenitor **1-F**, is contained within a 4,5-diamidofluorene scaffold. The oxygen atom, formerly residing within the xanthene backbone, completes the coordination sphere around the boron centre as an oxido ligand, which is bridging to the [Li(THF)$_2$]$^+$ cation. The N–B–N angle of 124.9° is indicative of an sp^2 hybridised boron centre, with the short B–O bond length 1.313(4) Å indicating the B–O bond to possess some double bond character, which was confirmed by IR spectroscopy revealing the B–O stretch at 1320 cm^{-1} (calc. 1317 cm^{-1}).

Reduction of the bromo starting material **1-Br** with lithium at room temperature gave a near-identical result, with the same fluorene-based boryloxy isolated, but as the LiBr adduct (see SI).

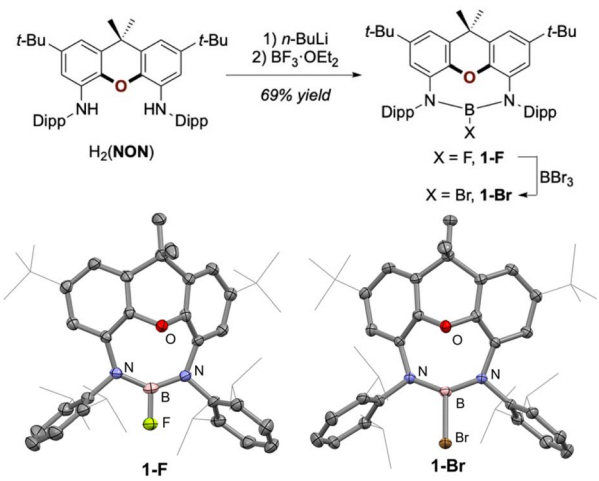

Fig. 2 (Top) synthesis of **1-F** and **1-Br** (Dipp: 2,6-diisopropylphenyl). (Bottom) molecular structure of **1-F** and **1-Br** as determined *via* X-ray crystallography. Thermal ellipsoids set at 50% probability, hydrogen atoms omitted, and selected groups shown in wireframe for clarity.

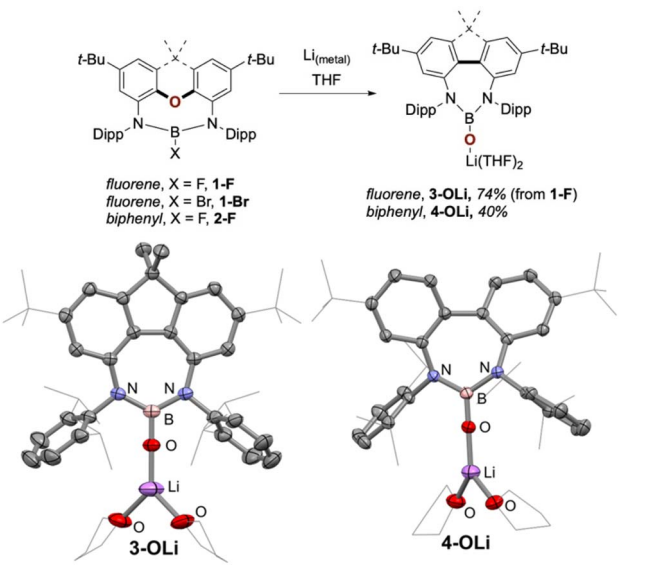

Fig. 3 (Top) reduction of boron halides **1-F**, **1-Br** and **2-F** with lithium, yielding the lithium boryloxy complexes **3-OLi** and **4-OLi**, respectively. (Bottom) molecular structure of **3-OLi** and **4-OLi** as determined by X-ray crystallography. Thermal ellipsoids set at 50% probability, hydrogen atoms omitted, and selected groups shown in wireframe for clarity.

However, this reaction was lower-yielding and less selective than the reduction of **1-F**, with multiple by-products observed by NMR spectroscopy.

With the *O*-deletion of **1-F** and **1-Br** confirmed, we wanted to investigate how important the cyclic nature of the xanthene-based ether was to this reaction. In recent work, we reported the synthesis of the "acyclic" substituted diphenylether-based equivalents of **1-F** and **1-Br** (**2-F** and **2-Br**).[19] Furthermore, we showed that the reduction of **2-Br** with lithium metal at −80 °C leads to *C*,*N*-bond-cleavage and a 1,2-migration of one Dipp group to the boron atom.[19] Gratifyingly, when the reduction of **2-F** was carried out under the same conditions as for **1-F** and **1-Br**, the lithium boryloxy *O*-deletion product **4-OLi** was isolated, albeit in lower yields than the fluorene analogue.

X-ray diffraction analysis of **4-OLi** revealed a strikingly similar molecular structure to **3-OLi** (Fig. 3). The biggest difference is found in the dihedral angle between the two aromatic rings of the fluorene motif in **3-OLi** (3.3°) and those in the biphenyl motif in **4-OLi** (39.8°), which aligns with the rigidity of the fluorene, forcing the backbone to adopt a planar geometry. To the best of our knowledge, this is the first report of an *O*-deletion reaction of amidoxanthene/diphenyl ethers, and the first report of diamidofluorene coordination complexes.[33] Noteworthy is that the reverse reaction, *O*-insertion, has recently been reported to occur biochemically in insects on related substrates.[34]

Mechanistic studies

To shine light on the underlying mechanism of the *O*-deletion reaction, extensive computational studies were carried out on the xanthene system at the BP86-D3BJ-CPCM(THF)/6–311++G**//BP86-D3BJ/6-31G** level of theory. Taking inspiration from the mechanistic investigations of Frenking, Driess, and coworkers (*vide supra*),[17,18] we initiated our mechanistic investigations by assuming that a closed-shell B(I) anion (boryl anion) was being generated from a two-electron reduction of the starting material (**1-F** or **1-Br**). However, in all mechanisms calculated (monomeric and dimeric, with or without including a lithium cation), at least one implausible step with an extraordinarily high barrier was located (see SI for further details). This led us to reconsider our starting point and whether only a single-electron reduction of the starting material was responsible for the transformation. Boron(II) radical (boranyl) species have seen use in a number of different synthetic reactions, such as alkyl halide cross couplings and radical additions to multiple bonds.[35] However they can be highly unstable, and so have only been isolated with coordination of an ancillary Lewis basic ligand.[35]

Starting from the open-shell B(II) radical compound **(NON)B$^{\bullet}$**, generated *via* a single-electron reduction of **1-F** or **1-Br**, a viable mechanism was calculated (Fig. 4). The first step involves coordination of the oxygen in the xanthene backbone to the B(II) centre (**INT1**), which proceeds through the low-energy transition state **TS0-1** (4.4 kcal mol^{-1}). In the next step, the radical is transferred from the boron(II) centre to one of the phenyl rings of the xanthene *via* **TS1-2** (15.3 kcal mol^{-1}), breaking a C–O bond and forming the aryl-centred radical intermediate (**INT2**). After rotating the aryl radical behind the plane of the aryloxy ring in a wagging motion through another low-energy transition state **TS2-3** (5.0 kcal mol^{-1}), the stage is set within **INT3** for the key C–C bond formation and C–O cleavage (**TS3-4**), which is the rate-determining step with a barrier of *ca.* 19.5 kcal mol^{-1}. This yields the oxidaneylborane radical product **(*N*,*N*)BO$^{\bullet}$** in a strongly exergonic step (−92.2 kcal mol^{-1}). Finally, in the reaction mixture, **(*N*,*N*)BO$^{\bullet}$** is

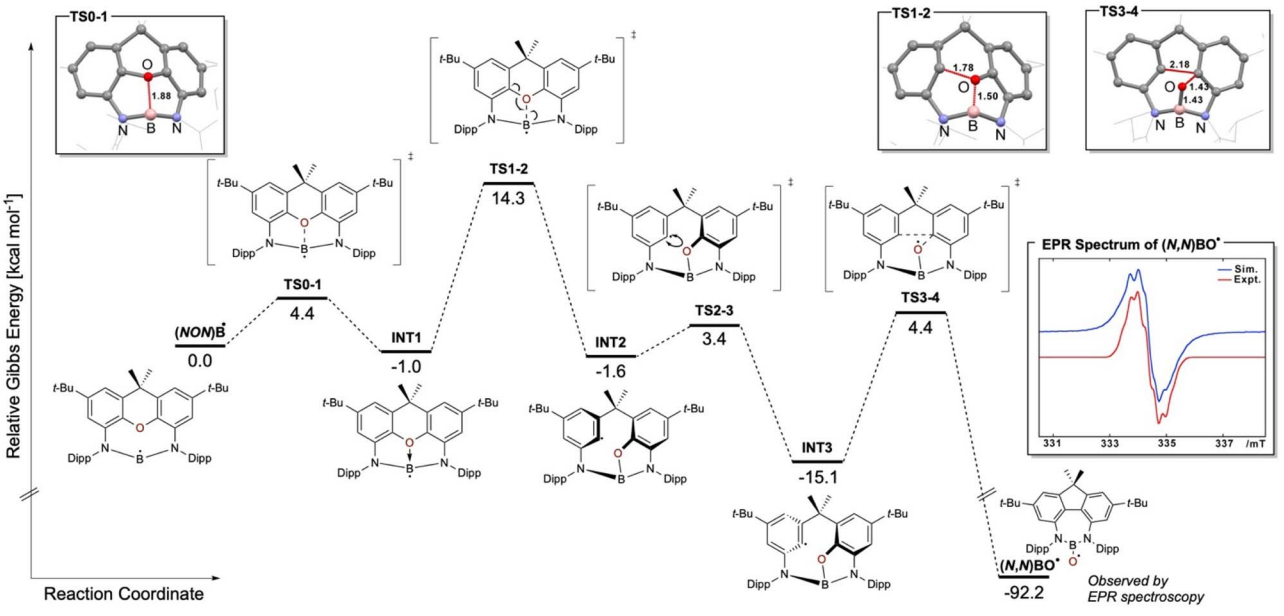

Fig. 4 Gibbs free energy profile (BP86-D3BJ-CPCM(THF)/6–311++G**//BP86-D3BJ/6–31G**) for the *O*-deletion reaction leading to **3-OLi**. Relative free energies are shown in kcal mol^{-1}. Inserts include models of the most important transition states with key distances shown in Å, and the acquired EPR spectrum of **(N,N)BO$^{\bullet}$** (red) along with its modelled spectrum (blue, see SI for full details).

converted into the isolated lithium boryloxy product **3-OLi** *via* a further one-electron reduction with lithium metal.

This open-shell mechanism contrasts with the closed-shell mechanism reported for **IV**.[18] However, in the reported study, an extraordinarily high barrier of +53.7 kcal mol^{-1} was calculated for one step, with the authors stating that the barrier does not agree with their experimental observations. In our case, an activation energy of ~20 kcal mol^{-1} is in line with our experimental observations. Furthermore, additional evidence for this radical mechanism was acquired through EPR spectroscopy. The reduction of **1-Br** was repeated, but after *ca.* 5 minutes of stirring at room temperature, an aliquot of the reaction mixture was removed and analysed by EPR spectroscopy. The EPR spectrum of the reaction solution revealed the presence of an open-shell species with hyperfine coupling consistent with the boryloxy radical **(*N,N*)BO˙** (Fig. 4), further supporting the open-shell mechanism presented (see SI for further details).

[1,3,2]Diazaborepin-2-ol

The boryloxy compounds **3-OLi** or **4-OLi** are moisture-sensitive, with exposure to air yielding quantitative amounts of the protonated products **3-OH** or **4-OH**, rare examples of [1,3,2] diazaborepin-2-ol derivatives. Both compounds were crystallographically characterised (Fig. 5).

3-OH or **4-OH** were found to be remarkably stable, showing no signs of decomposition even when treated with hot triflic acid, boiling lithium hydroxide solution, or KHF_2, amongst others. However, under forcing conditions, the OH group of 3-OH can be substituted with fluoride by treating the compound with neat BF3·OEt2 (10 equiv.) and heating to 100 °C over 48 hours, yielding the boron fluoride **3-F** in a 50% isolated yield.

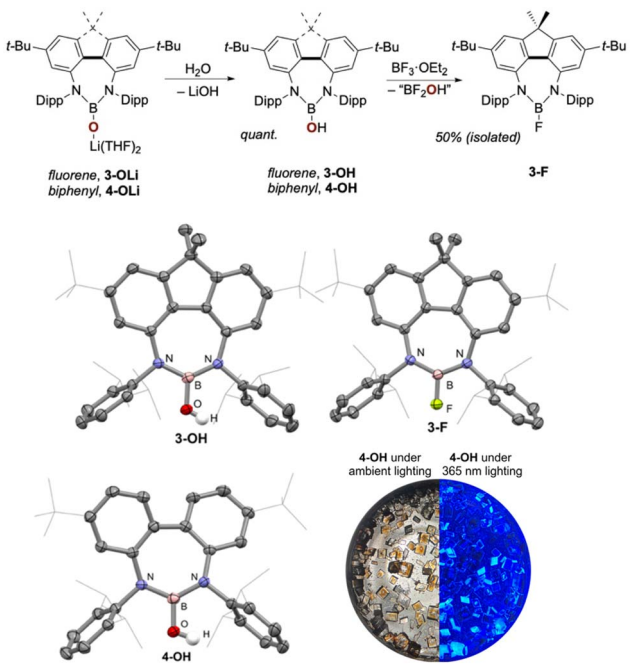

Fig. 5 (Top) hydrolysis of boryloxy compounds to give borinic acid products 3-OH and 4-OH, along with the synthesis of 3-F. (Middle and bottom) molecular structures of 3-OH, 3-F and 4-OH as determined *via* X-ray crystallography. Thermal ellipsoids set at 50% probability, most hydrogen atoms omitted, and selected groups shown in wire-frame for clarity. Insert: Crystals of 4-OH under ambient and 365 nm light, respectively (photos taken through a polarisation filter).

Table 1 Absorption and emission characteristics of 3-OH, 3-F, and 4-OH measured from diluted toluene solutions at room temperature (excitation wavelength set at 350 nm)

	Absorption λ_{abs}/nm	Emission λ_{em}/nm	τ/ns	Φ
3-OH	357, 376	385, 407	5.70	0.59
3-F	300, 358, 377	388, 409	7.03	0.40
4-OH	339	422	6.37	0.50

Photophysical properties

Working with these [1,3,2]diazaborepin compounds (**3-OH**, **3-F**, and **4-OH**), it was immediately evident that they were highly emissive compounds. Upon irradiation of a crystalline sample of **3-OH** with a UV torch (365 nm), intense blue emission is observed (Fig. 5). As such, the photophysical properties of **3-OH**, **3-F**, and **4-OH** were measured both in solution and in solid-state, and the results are summarised in Table 1. The absorption profiles measured from diluted toluene solutions (Fig. S30) reveal broad bands in the lower-energy UV region between 300 and 400 nm. These are ascribed to ππ* electronic transitions. Notably, the absorption spectra of **3-OH** and **3-F** appear more structured in the 350–400 nm region, consistent with the enhanced rigidity of the fluorene moiety compared with the more flexible biphenyl in **4-OH**. Upon excitation at 350 nm, all three compounds appear blue/aqua luminescent in both solution and the solid state at room temperature. The emission spectra from diluted toluene solutions are very similar (Fig. S31), displaying broad bands between 400 and 550 nm, characterised by a vibronic structure typical of ππ* excited states. On the other hand, the emission profiles recorded from solid-state samples (Fig. S32) show a slight blueshift, attributed to the absence of solvent stabilisation of the excited states, without evidence of extensive aggregation. The excited state lifetime decays τ were satisfactorily fitted by monoexponential functions, revealing relatively short decays in the 5.70–7.03 ns range, typical of spin-allowed fluorescent emission (Table 1). Measurement of photoluminescent quantum yields (Φ) in the 40–59% range demonstrates that these compounds exhibit strong emission and are comparable to those of boron-dipyrromethene scaffolds (BODIPY).[36] Given the wide range of applications that BODIPY-type species have found, we propose that these compounds could serve as a new, accessible class of fluorophores. Notably, the similarities of photophysical properties of **3-OH**, **3-F**, and **4-OH** would suggest that this class of fluorophores are highly tunable, and that physico-chemical properties can be optimised independently from photophysical properties.

Aluminium

The stability of the [1,3,2]diazaborepin compounds is beneficial for their potential future uses as fluorophores, but for the broader applicability of the *O*-deletion reaction in organic

synthesis, removal of the organic fragment from the group 13 element would be beneficial. During this work, the removal of the boron centre from **3-OH**, **3-F**, and **4-OH** to give the 4,5-substituted organic product was extensively investigated, but without success (see SI for details). Therefore, it was concluded that to liberate the newly C–C coupled organic diamine, an element other than boron would be required. Aluminium, being the element below boron in group 13, and with Al–N bonds much more susceptible to hydrolysis,[37] was an obvious choice. However, the reduction of (**NON**)AlI (the aluminium analogue of **1-F**/**1-Br**) has been extensively studied – producing Al(I) aluminyl anions and the Al(II) dialane – with no evidence of an *O*-deletion reaction.[38] Aluminium(II) radicals have been reported several times, and can be capable of significant reactivity,[39] however these results suggest that the Al(II) radical intermediate may be too stable to potentially achieve a similar *O*-deletion reaction. Therefore, to achieve comparable reactivity, the radical intermediate would need to be destabilised.

In recent work, we reported ^{tBu}**NON**, where the flanking aryl groups of **NON** have been replaced with more electron-donating *tert*-butyl groups.[38] Stirring a solution of AlI(^{tBu}**NON**) (**5**) over excess KC_8 at 50 °C overnight gives an analogous *O*-deletion reaction, from which the crystalline potassium 'aloxy' complex **6** can be isolated. The structure of **6** was confirmed by X-ray diffraction (Fig. 6) and consists of an Al_2O_2 core, in which each of the aluminium centres is coordinated by one diamidofluorene ligand. The charge is compensated by two potassium atoms that connect the two fluorene backbones *via* arene-π interactions. EPR spectroscopic analysis of the reaction solution indicates the presence of an open-shell intermediate,

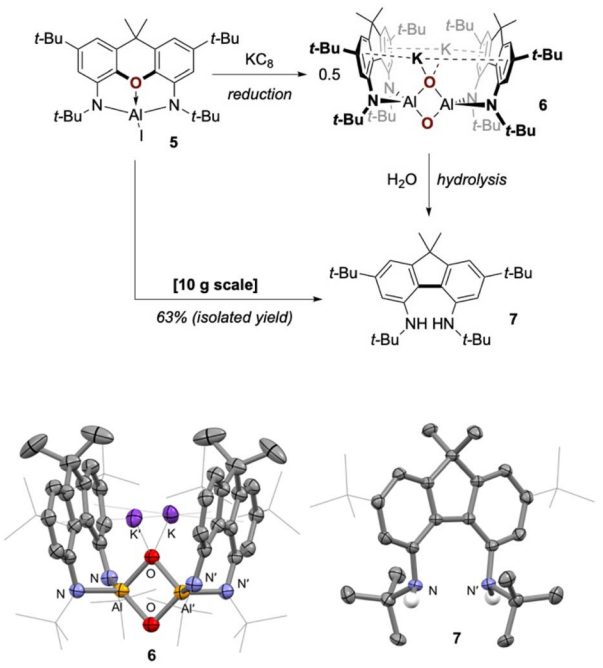

Fig. 6 (Top) synthesis of **6** and **7**. (Bottom) molecular structures of **6** and **7** as determined *via* X-ray crystallography. Thermal ellipsoids are set at 50% probability, most hydrogen atoms omitted, and selected groups are shown in wireframe for clarity.

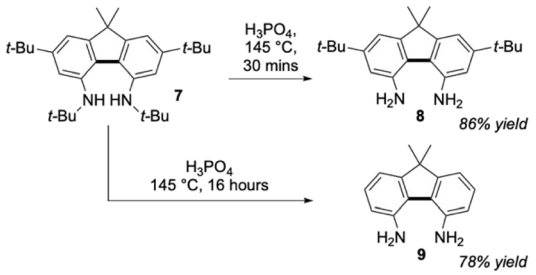

Fig. 7 De-*tert*-butylation of **7** with phosphoric acid to give **8** and **9**.

consistent with a radical mechanism analogous to that proposed for the boron system (see SI for details).

Exposure of **6** to air results in complete hydrolysis of the product, yielding the metal-free 4,5-diaminofluorene (**7**) in quantitative yield. To demonstrate the feasibility of this procedure in the large-scale synthesis of 4,5-diaminofluorenes, the reaction was repeated on a 10 g scale. A simple organic workup (in air) followed by recrystallisation gave the 4,5-diaminofluorene **7** in 63% yield (Fig. 6).

Finally, the *N*-bound *tert*-butyl groups on **7** can be easily removed by heating the compound in phosphoric acid (85%-wt) to 145 °C for 30 minutes. This gives the primary 4,5-diaminofluorene (**8**) in an 86% yield (Fig. 7). Conveniently, heating the same reaction for longer periods (16 hours) leads to complete de-*tert*-butylation of the compound, also removing the *tert*-butyl groups at the 2,7 positions of the fluorene, affording the unsubstituted 4,5-diaminofluorene (**9**) in 78% yield (Fig. 7). This represents the first high-yielding, concise, and reproducible synthesis of 4,5-diaminofluorenes, a class of compounds that have been barely studied due to synthetic inaccessibility,[40–43] opening the door to broad future applications.

Conclusions

In summary, we have developed a selective and scalable *O*-deletion strategy for diarylether frameworks mediated by boron and aluminium radicals, enabling direct skeletal editing *via* formal oxygen removal and concomitant C–C bond formation. Reduction of diamido-xanthene and diphenylether boron complexes proceeds through a transient open-shell B(II) intermediate, furnishing lithium boryloxy species in high yield and on a multigram scale. Subsequent hydrolysis provides previously inaccessible fluorene- and biphenyl-based [1,3,2] diazaborepin-2-ols, which exhibit remarkable chemical robustness and high photoluminescence quantum yields, identifying them as a new, tunable class of boron-containing fluorophores.

Extension of this chemistry to aluminium sees a similar *O*-deletion reaction, which is proposed to occur *via* an analogous Al(II) radical mechanism. In this case, the compound is readily hydrolysed, enabling the clean isolation of the metal-free N^4,N^5,2,7-tetra-*tert*-butyl-9,9-dimethyl-4,5-diaminofluorene (**7**). The compound can be partially or fully de-*tert*-butylated with hot phosphoric acid, giving the primary amine compounds **8** and **9**. The compounds are expected to serve as versatile

precursors to a previously inaccessible series of 4,5-diaminofluorene compounds in molecule synthesis and materials chemistry.

Author contributions

E. N. performed most of the synthetic work and more routine characterisation. G. R. N. performed the computational work under the supervision of C. L. M. E. D. performed the photophysical measurements under the supervision of M. M. L. F. L. was responsible for the EPR collection and modelling, supervised by N. C. F. K. performed some synthetic work and was responsible for project management. J. H. was responsible for funding acquisition and providing resources. All authors were involved in reviewing and editing the manuscript.

Conflicts of interest

There are no conflicts to declare.

Data availability

CCDC 2514982–2514992 and 2515042 contain the supplementary crystallographic data for this paper.[44a–l]

The data supporting this article have been included as part of the supplementary information (SI). Supplementary information: synthetic and characterisation data, including those for crystallographic, EPR, photophysical and computational studies. See DOI: https://doi.org/10.1039/d6sc01056c.

Acknowledgements

JH would like to thank the Australian Research Council (FT240100229) for the funding of this work. This research was undertaken with the assistance of resources from the National Computational Infrastructure (NCI Australia), an NCRIS enabled capability supported by the Australian Government, and the University of Bath's Research Computing Group (https://doi.org/10.15125/b6cd-s854) for their support of this work.

Notes and references

1 J. Jurczyk, J. Woo, S. F. Kim, B. D. Dherange, R. Sarpong and M. D. Levin, *Nat. Synth.*, 2022, **1**, 352.
2 K. R. Campos, P. J. Coleman, J. C. Alvarez, S. D. Dreher, R. M. Garbaccio, N. K. Terrett, R. D. Tillyer, M. D. Truppo and E. R. Parmee, *Science*, 2019, **363**, 244.
3 F.-P. Wu, J. L. Tyler and F. Glorius, *Acc. Chem. Res.*, 2025, **58**, 893.
4 A. R. Fout, B. C. Bailey, J. Tomaszewski and D. J. Mindiola, *J. Am. Chem. Soc.*, 2007, **129**, 12640.
5 A. R. Fout, B. C. Bailey, D. M. Buck, H. Fan, J. C. Huffman, M.-H. Baik and D. J. Mindiola, *Organometallics*, 2010, **29**, 5409.
6 A. Conboy and M. F. Greaney, *Chem*, 2024, **10**, 1940.
7 Q. Cheng, D. Bhattacharya, M. Haring, H. Cao, C. Mück-Lichtenfeld and A. Studer, *Nat. Chem.*, 2024, **16**, 741.
8 T. J. Pearson, R. Shimazumi, J. L. Driscoll, B. D. Dherange, D.-I. Park and M. D. Levin, *Science*, 2023, **381**, 1474.
9 A. Fanourakis, Y. Ali, L. Chen, P. Q. Kelly, A. J. Bracken, C. B. Kelly and M. D. Levin, *Nature*, 2025, **641**, 646.
10 S. H. Kennedy, B. D. Dherange, K. J. Berger and M. D. Levin, *Nature*, 2021, **593**, 223.
11 P. Schorigin, *Ber. dtsch. Chem. Ges. A/B*, 1923, **56**, 176.
12 P. Schorigin, *Ber. dtsch. Chem. Ges. A/B*, 1924, **57**, 1627.
13 P. A. Sartoretto and F. J. Sowa, *J. Am. Chem. Soc.*, 1937, **59**, 603.
14 F. C. Weber and F. J. Sowa, *J. Am. Chem. Soc.*, 1938, **60**, 94.
15 H. Gilman and J. Dietrich, *J. Org. Chem.*, 1957, **22**, 851.
16 M. Lissel, J. Kottmann, D. Tamarkin and M. Rabinovitz, *Z. Naturforsch. B*, 1988, **43**, 1211.
17 J. Fan, J. Xu, Q. Ma, S. Yao, L. Zhao, G. Frenking and M. Driess, *J. Am. Chem. Soc.*, 2024, **146**, 20458.
18 J. Fan, S. Pan, S. Yao, C. Ding, G. Frenking and M. Driess, *J. Am. Chem. Soc.*, 2025, **147**, 6925.
19 E. E. Nahon, G. R. Nelmes, P. J. Brothers and J. Hicks, *Chem. Commun.*, 2023, **59**, 14281.
20 J. Hicks, M. Juckel, A. Paparo, D. Dange and C. Jones, *Organometallics*, 2018, **37**, 4810.
21 Y. K. Loh, L. Ying, M. Ángeles Fuentes, D. C. H. Do and S. Aldridge, *Angew. Chem., Int. Ed.*, 2019, **58**, 4847.
22 Y. K. Loh, K. Porteous, M. Á. Fuentes, D. C. H. Do, J. Hicks and S. Aldridge, *J. Am. Chem. Soc.*, 2019, **141**, 8073.
23 L. Weber, *Coord. Chem. Rev.*, 2021, **431**, 213667.
24 D. Sarkar, P. Vasko, T. Gluharev, L. P. Griffin, C. Bogle, J. Struijs, J. Tang, A. F. Roper, A. E. Crumpton and S. Aldridge, *Angew. Chem., Int. Ed.*, 2024, **63**, e202407427.
25 D. Sarkar, P. Vasko, A. F. Roper, A. E. Crumpton, M. M. D. Roy, L. P. Griffin, C. Bogle and S. Aldridge, *J. Am. Chem. Soc.*, 2024, **146**, 11792.
26 D. Sarkar, P. Vasko, L. Ying, J. J. C. Struijs, L. P. Griffin and S. Aldridge, *Angew. Chem., Int. Ed.*, 2025, **64**, e202502326.
27 R. Guthardt and C. Jones, *Chem. Commun.*, 2024, **60**, 1583.
28 C. Helling, D. J. D. Wilson and C. Jones, *J. Am. Chem. Soc.*, 2025, **147**, 16620.
29 C. Wei, L. Guo, C. Zhu and C. Cui, *Angew. Chem., Int. Ed.*, 2025, **64**, e202414464.
30 L. R. Thomas-Hargreaves, D. Hunger, M. Kern, A. J. Wooles, J. Van Slageren, N. F. Chilton and S. T. Liddle, *Chem. Commun.*, 2021, **57**, 733.
31 X. Dan, J. Du, S. Zhang, J. A. Seed, M. Perfetti, F. Tuna, A. J. Wooles and S. T. Liddle, *Inorg. Chem.*, 2024, **63**, 9588.
32 J. T. Boronski, L. R. Thomas-Hargreaves, M. A. Ellwanger, A. E. Crumpton, J. Hicks, D. F. Bekiş, S. Aldridge and M. R. Buchner, *J. Am. Chem. Soc.*, 2023, **145**, 4408.
33 Oxygen extrusion has been observed in the decamethylcobaltocene mediated reduction of strained dinaphthooxepine bisimides(*a*) M. Odajima, N. Fukui and H. Shinokubo, *Org. Lett.*, 2023, **25**, 282 and the reductive deoxygenation of ethers *via* nickel catalysis in the presence of reductants; (*b*) Z. C. Cao and Z. J. Shi, *J. Am. Chem. Soc.*, 2017, **139**, 6546, through photochemical rearrangement of

diphenyl ethers; (*c*) N. Haga and H. Takayanagi, *J. Org. Chem.*, 1996, **61**, 735, and recently from oxepines using AFM tip chemistry; (*d*) S. Mishra, V. Malave, R. Svensson, H. Grönbeck, F. Albrecht, D. Peña and L. Gross, *J. Am. Chem. Soc.*, 2025, **147**, 44055, and in the cobalt-catalysed transformation of various ethers into 1,2-diarylethanes:; (*e*) M. K. Sahu, S. Pattanaik, G. Joshi, E. D. Jemmis and C. Gunanathan, *Angew. Chem., Int. Ed.*, 2026, **65**, e20176. Other examples are included in the perspective on unimolecular fragment coupling; (*f*) R. Shimazumi and M. Tobisu, *JACS Au*, 2024, **4**, 1676.

34 A. Usami, H. Kono, V. Austen, Q. M. Phung, H. Shudo, T. Kato, H. Yamada, A. Yagi, K. Amaike, K. J. Fujimoto, T. Yanai and K. Itami, *Science*, 2025, **388**, 1055.

35 Some reviews and select examples of boryl radicals and their reactivity(*a*) T. Taniguchi, *Chem. Soc. Rev.*, 2021, **50**, 8995; (*b*) X. Guo and Z. Lin, *Chem. Sci.*, 2024, **15**, 3060; (*c*) Y. Su and R. Kinjo, *Coord. Chem. Rev.*, 2017, **352**, 346; (*d*) T. Taniguchi, *Eur. J. Org Chem.*, 2019, **2019**, 6308; (*e*) Z. Zhang, M. J. Tilby and D. Leonori, *Nat. Synth.*, 2024, (3), 1221.

36 (*a*) A. Loudet and K. Burgess, *Chem. Rev.*, 2007, **107**, 4891; (*b*) G. Ulrich, R. Ziessel and A. Harriman, *Angew. Chem., Int. Ed.*, 2008, **47**, 1184; (*c*) H. Lu, J. Mack, Y. Yang and Z. Shen, *Chem. Soc. Rev.*, 2014, **43**, 4778; (*d*) Y. Ni and J. Wu, *Org. Biomol. Chem.*, 2014, **12**, 3774; (*e*) T. Kowada, H. Maeda and K. Kikuchi, *Chem. Soc. Rev.*, 2015, **44**, 4953; (*f*) J. Bañuelos-Prieto and R. Sola Llano, *BODIPY Dyes - A Privilege Molecular Scaffold with Tunable Properties*, IntechOpen, 2019; (*g*) V. I. Martynov and A. A. Pakhomov, *Russ. Chem. Rev.*, 2021, **90**, 1213; (*h*) N. A. Bumagina and E. V. Antina, *Coord. Chem. Rev.*, 2024, **505**, 215688.

37 D. R. Lide, *CRC Handbook of Chemistry and Physics*, CRC Press, Boca Raton, FL, 1974.

38 F. Kallmeier, A. J. R. Matthews, G. R. Nelmes, N. R. Lawson and J. Hicks, *Dalton Trans.*, 2024, **53**, 12450.

39 Some reviews and select examples of aluminyl radicals and their reactivity(*a*) R. P. Singh and N. P. Mankad, *JACS Au*, 2025, **5**, 2076; (*b*) M. Nakamoto, T. Yamasaki and A. Sekiguchi, *J. Am. Chem. Soc.*, 2005, **127**, 6954; (*c*) D. Mandal, T. I. Demirer, T. Sergeieva, B. Morgenstern, H. T. A. Wiedemann, C. W. M. Kay and D. M. Andrada, *Angew. Chem., Int. Ed.*, 2023, **62**, e202217184.

40 E. K. Weisburger and J. H. Weisburger, *J. Org. Chem.*, 1955, **20**, 1396.

41 E. Weisburger, *J. Org. Chem.*, 1956, **21**, 698.

42 H. A. Staab, T. Saupe and C. Krieger, *Angew Chem. Int. Ed. Engl.*, 1983, **22**, 731.

43 O. V. Semidetko, L. A. Chetkina, V. K. Bel'skii, A. N. Poplavskii, A. M. Andrievskii and K. M. Dyumaev, *J. Struct. Chem.*, 1988, **29**, 330.

44 (*a*) CCDC 2514982: Experimental Crystal Structure Determination, 2026, DOI: 10.5517/ccdc.csd.cc2qf1gp; (*b*) CCDC 2514983: Experimental Crystal Structure Determination, 2026, DOI: 10.5517/ccdc.csd.cc2qf1hq; (*c*) CCDC 2514984: Experimental Crystal Structure Determination, 2026, DOI: 10.5517/ccdc.csd.cc2qf1jr; (*d*) CCDC 2514985: Experimental Crystal Structure Determination, 2026, DOI: 10.5517/ccdc.csd.cc2qf1ks; (*e*) CCDC 2514986: Experimental Crystal Structure Determination, 2026, DOI: 10.5517/ccdc.csd.cc2qf1lt; (*f*) CCDC 2514987: Experimental Crystal Structure Determination, 2026, DOI: 10.5517/ccdc.csd.cc2qf1mv; (*g*) CCDC 2514988: Experimental Crystal Structure Determination, 2026, DOI: 10.5517/ccdc.csd.cc2qf1nw; (*h*) CCDC 2514989: Experimental Crystal Structure Determination, 2026, DOI: 10.5517/ccdc.csd.cc2qf1px; (*i*) CCDC 2514990: Experimental Crystal Structure Determination, 2026, DOI: 10.5517/ccdc.csd.cc2qf1qy; (*j*) CCDC 2514991: Experimental Crystal Structure Determination, 2026, DOI: 10.5517/ccdc.csd.cc2qf1rz; (*k*) CCDC 2514992: Experimental Crystal Structure Determination, 2026, DOI: 10.5517/ccdc.csd.cc2qf1s0; (*l*) CCDC 2515042: Experimental Crystal Structure Determination, 2026, DOI: 10.5517/ccdc.csd.cc2qf3dp.